

IMPEDANCE MODEL FOR THE FERMILAB RECYCLER RING

B. C. Gladwyn*, University of Cambridge, Cambridge, UK

O. Mohsen, Argonne National Laboratory, Lemont, IL, USA

R. Ainsworth, Fermi National Accelerator Laboratory, Batavia, IL, USA

M.K. Duncan, The University of Chicago, Chicago, IL, USA

Abstract

We present an impedance model of the Fermilab Recycler ring in PyHEADTAIL. The model uses analytical expressions for the wakefields of beamline components that contribute significantly to the impedance. The effect of indirect space-charge is included as an inductive impedance. Benchmarking against coherent Betatron tune shifts, the impedance model is found to capture 73.4% of the observed tune shifts. Our findings serve as a stepping stone for the development of a realistic impedance model crucial for studying impedance-driven instabilities at higher intensity.

INTRODUCTION

The Proton Improvement Plan-II (PIP-II) [1] is Fermilab's plan to push the intensity frontier. For the Recycler Ring, [2–6] the upgrade may require accumulating 50% more beam than under current operation [7]. With high-intensity operation making impedance-driven instabilities more of a concern [8, 9], a realistic impedance model [10, 11] is a useful tool to identify major impedance contributions and predict beam instability thresholds [12]. We develop a model in PyHEADTAIL using analytical expressions for the wakefields generated by beamline components and include the effect of indirect space-charge impedance with a broadband inductive impedance [13]. The model is benchmarked with coherent betatron tune shifts and found to account for 73.4% of the observed tune shift. This work serves as a foundation for the development of a realistic impedance model of the Fermilab Recycler.

IMPEDANCE AND WAKE

Impedance characterizes the effect of the wakefields generated by a ‘source’ particle on a trailing ‘test’ particle [14, 15]. The force experienced by a ‘test’ particle trailing by a distance s , averaged over a circumference ($C \equiv 2\pi R$) and normalized by source and test charge e , is the wake function $W_y(z)$

$$W_y(z) = \frac{2\pi R}{e^2} F(x_{\text{test}}, y_{\text{test}}, s) \quad (1)$$

$$= -\frac{i}{2\pi} \int_{-\infty}^{\infty} d\omega e^{i\omega s/\nu} Z_y(\omega), \quad (2)$$

where $F(x_{\text{test}}, y_{\text{test}}, s)$ is the force on the test particle, and the impedance $Z_y(\omega)$ has been defined as the Fourier transform of the wake function. Impedances and wake functions depend solely on the beam surroundings [13]. We consider

ultra-relativistic wakes, for which $W(z) = 0$ for $z < 0$ to enforce causality.

Betatron tune shifts are proportional to the effective impedance given by [13]

$$(Z_1^\perp)_{\text{eff}} = \frac{\sum_{p=-\infty}^{\infty} Z_1^\perp(\omega') h_l(\omega' - \omega_\xi)}{\sum_{p=-\infty}^{\infty} h_l(\omega' - \omega_\xi)}, \quad (3)$$

where $\omega' = p\omega_0 + \omega_\beta + l\omega_s$ and $\omega_\xi = \xi\omega_\beta/\eta$, revolution frequency ω_0 , betatron oscillation frequency ω_β , synchrotron frequency ω_s , chromaticity ξ and slippage factor η . For a Gaussian bunch we have the mode $h_l(\omega) = (\omega\sigma/c)^{2l} \exp(-\omega^2\sigma^2/c^2)$.

SPACE-CHARGE TUNE SHIFT

Indirect space-charge (image force) contributes to the total coherent tune shift [14, 15].¹ The magnitude of this contribution can be calculated with [16]

$$\Delta\nu_{\text{coh}}^{V,H} = -\frac{Nr_0R}{\pi\gamma\beta^2\nu_0^{V,H}} \left[\frac{1-\chi_e}{B} \frac{\xi_1^{V,H}}{h^2} + \mathcal{F}\beta^2 \frac{\epsilon_2^{V,H}}{g^2} - \frac{\beta^2(\xi_1^{V,H} - \epsilon_1^{V,H})}{h^2} - \beta^2 \left(\frac{1}{B} - 1 \right) \frac{\xi_1^{V,H}}{h^2} \right], \quad (4)$$

where N is the number of protons, r_0 is the classical proton radius, χ_e is the neutralization coefficient, B is the bunching factor, \mathcal{F} is the fraction of the ring sandwiched between dipole magnets, g the magnet half-gap and h the pipe ‘radius’. The Laslett coefficients $\xi_1^{V,H}$, $\epsilon_1^{V,H}$ and $\epsilon_2^{V,H}$ incorporate the elliptical shape of the beam pipe into the analysis [17]. The single bucket bunching factor $B = \sqrt{2\pi} f_{rf} \sigma_z$ for $f_{rf} = h_r f_0$ with harmonic number h_r and revolution frequency f_0 [18].

WAKE FUNCTIONS

It is known that the primary contributions to the Recycler's impedance are from the resistive wall, indirect space-charge, Beam Position Monitors (BPMs) and kickers [19]. Those impedances can be calculated analytically; see [20]. We present the results and give the parameters relevant to the Fermilab Recycler.

Resistive Wall

The m^{th} azimuthal transverse impedance for a circular resistive wall with $\delta_{\text{skin}} = \sqrt{2/\sigma_c \omega \mu_r \mu_0} = 1.07/\sqrt{\omega} \ll t$ for

¹ Direct space-charge (self-force) does not contribute as an impedance and only gives incoherent tune shifts.

* bengladwyn@btinternet.com

wall thickness t , conductivity σ_c and relative permeability μ_r is given by

$$Z_m^\perp = \frac{Lc}{\omega\pi\sigma_c\delta_{\text{skin}}b^{2m+1}} \frac{1 - \text{sgn}(\omega)}{1 + \delta_{0m}}, \quad (5)$$

where b is the pipe radius. We need only to consider $m = 1$. For $b\chi \gg |z| \approx c|\omega| \gg b\chi^{1/3}$ where $\chi = 1/(Z_0\sigma_c b)$ the transverse dipolar wake function becomes

$$W_m = -\frac{c}{\pi b^{2m+1}(1 + \delta_{0m})} \sqrt{\frac{Z_0}{\pi\sigma_c}} \frac{L}{|z|^{1/2}}. \quad (6)$$

However, the Fermilab Recycler has an elliptical beam pipe with half width $w = 3.75''$ and $h = 1.75''$. Yokoya form factors found from [21] can be multiplied by the circular resistive wall wakes to find the dipole and quadrupole wakes. They are shown in Table 1 with other relevant parameters.

Table 1: Resistive Wall Parameters

Parameter	Value
Y_{dip}^y	0.843
Y_{quad}^y	0.377
Y_{dip}^x	0.460
Y_{quad}^x	-0.395
b	0.0222 m
σ_c	1.35×10^6 S m ⁻¹
L	3319 m

Beam Position Monitors

A pair of strip-line BPMs of length L_{BPM} each subtending to pipe axis ϕ_0 and terminated with an impedance Z_c at the upstream end has transverse impedance

$$Z_1^\perp = \left[\frac{Z_0^\parallel}{\omega} \right]_{\text{pair}} \frac{c}{b^2} \left(\frac{4}{\phi_0} \right)^2 \sin^2 \frac{\phi_0}{2}, \quad (7)$$

$$Z_0^\parallel = 2Z_c \left[\frac{\phi_0}{2\pi} \right]^2 \left[2 \sin^2 \frac{\omega L_{\text{BPM}}}{c} - i \sin \frac{2\omega L_{\text{BPM}}}{c} \right]. \quad (8)$$

The corresponding transverse wake function is

$$W_1 = \frac{8Z_c c}{\pi^2 b^2} \sin^2 \frac{\phi_0}{2} [H(z) - H(z + 2L)]. \quad (9)$$

The Recycler has 205 sets of horizontal BPMs and 205 sets of vertical BPMs of $L_{\text{BPM}} = 12''$, $\phi_0 = \pi$ and $Z_c = 50 \Omega$.

Kickers

The Recycler has 7 kickers. Their impedance has been measured directly [22] to be $-0.2M\Omega\text{m}^{-1}$, falling off above 30MHz. We have modeled this impedance as a circular resonator with transverse impedance and wake given by

$$Z_m^\perp = \frac{c}{\omega} \frac{R_s}{1 + iQ \left(\frac{\omega_R}{\omega} - \frac{\omega}{\omega_R} \right)}, \quad (10)$$

$$W_m = \frac{R_s^m c \omega_r}{Q \bar{\omega}_r} e^{az/c} \sin \frac{\bar{\omega}_r z}{c}, \quad (11)$$

respectively. We have $\alpha = \omega_r/2Q$, $m = 1$ and $\bar{\omega}_r = \sqrt{|\omega_r^2 - \alpha^2|}$. We choose $Q = 1$, $\omega_r = 30$ MHz and $R_s = 2000 \Omega$.

Indirect Space-charge

We incorporate indirect space-charge using a δ -function wake function²

$$W_1^{\text{Indirect}}(z) = -\frac{Z_0 c L}{2\pi \gamma^2 h^2} \delta(z), \quad (12)$$

Since impedance is proportional to the inverse Fourier transform of the wake function, the indirect space-charge impedance must be a constant. The impedance is inductive (negative and imaginary) and is included by taking the limit $Q \rightarrow \infty$, $R_s \rightarrow \infty$ of a circular resonator such that R_s/Q is fixed (see [13]). From Eqs. (10) and (11) we have

$$Z_m^\perp \rightarrow -i \frac{c R_s}{Q \left(\omega_R - \frac{\omega^2}{\omega_R} \right)}, \quad (13)$$

$$W_m(z) = \frac{c R_s}{Q} \sin \frac{\omega_R z}{c}. \quad (14)$$

At low frequencies, this impedance becomes inductive $Z_m^\perp \rightarrow -i c R_s / Q \omega_R$. In our simulation, we use an inductive impedance with parameters that reproduce the tune shifts calculated using Eq. (4) and the parameters in Table 2.

$$W_m(z) = -\frac{c |R_s|}{Q} \sin \frac{\omega_R z}{c}. \quad (15)$$

Table 2: Coherent Tune Shift Parameters [23]

Parameter	Value
χ_e	0
$\xi_1^{\text{V,H}}$	0.6110, 0.0118
$\epsilon_2^{\text{V,H}}$	$\frac{\pi^2}{24}, -\frac{\pi^2}{24}$
$\epsilon_1^{\text{V,H}}$	0.1997, -0.1997
h_{rf}	28
f_0	89812 Hz
h	0.022 m

PYHEADTAIL SIMULATIONS

The estimated impedances are plotted in Fig. 1 along with the h_0 mode envelope. We incorporate these impedances into our PyHEADTAIL simulations by computing the wake for each impedance. We then use PyHEADTAIL simulation with the relevant wake to calculate the coherent tune shift for each impedance. Subsequently, our simulations include the sum of all the individual impedance components³.

² The δ -function is motivated by realizing that the space-charge force acts solely on an individual particle [13].

³ With all impedances included we find that the net tune shift is slightly smaller than the sum of the individual tune shifts due to partial cancellation of the wakes.

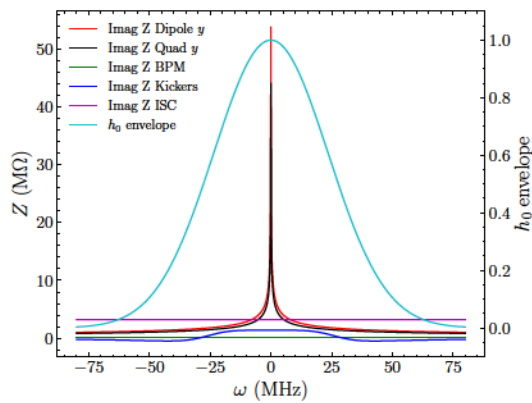


Figure 1: Contributions to the impedance of elliptical resistive wall, BPMs, kickers and indirect space-charge as a function of frequency.

To find the coherent tune shift, we track 1000 macroparticles for 8000 turns with the chromaticity set to zero. The average position of the particles is then Fourier transformed and the fractional tune is found by fitting a Gaussian to the resultant spectrum. This procedure is repeated for intensities N in range $5 \times 10^{10} - 5.5 \times 10^{11}$ protons per bunch (ppb).

The result of the individual contribution of each impedance source considered is depicted in Fig. 2 and it shows that the largest contribution of the impedance is due to the resistive wall.

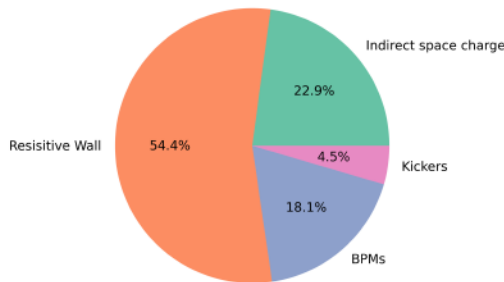


Figure 2: The relative magnitude of the contributions to the impedance for the sources considered.

BENCHMARKING

We benchmark our results by comparing our simulation with earlier coherent tune shift measurements in the Recycler ring. The measurements were performed using single bunches with similar bunch lengths ($\sigma_z \sim 26$ ns) and similar intensities used in our simulations. In the measurement, the tune shifts were determined by inspecting the bunch spectrum from the Fourier transform of a stripline BPM in the ring. Moreover, the measurements were performed with chromaticity values close to zero [24].

Comparing the tune shift from PyHEADTAIL and the experimental data, our simulations show that the impedance model accounts for 52% of the observed tune shift; see Fig. 3. However, PyHEADTAIL assumes a constant β_y for the whole circumference of the machine. Since the impedance

depends on the β_y function by [25]

$$Z_1^\perp \propto \frac{2\pi\nu_y}{C} \int_0^C \beta_y(s) ds = 1.37, \quad (16)$$

we must multiply the simulated tune shift (excluding the contribution from indirect space-charge) by this factor. After correction, the model accounts for 73.4% of the observed tune shift. This is in line with impedance estimates of typical impedance models [10].

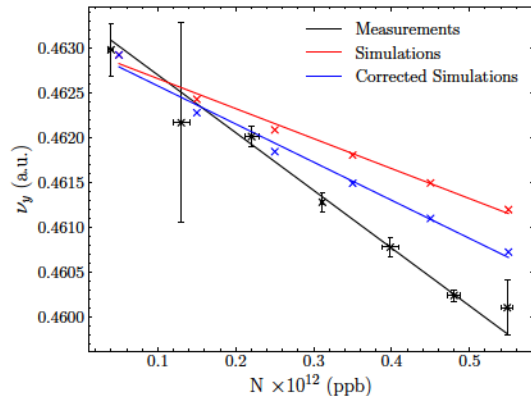


Figure 3: Fractional coherent tune shifts shown as a function of intensity for the measured data in our model.

CONCLUSIONS

An initial impedance model for the Fermilab Recycler ring was developed using PyHEADTAIL. Despite the simplifications and assumptions inherent in our approach, the model accounts for $\sim 73\%$ of the observed coherent betatron tune shifts. The model can be improved by including a more accurate computation of the resistive wall impedance since it is the largest contribution to our tune shift. For instance, a more complicated model calculated using Impedance Wake 2D is being considered [26]. Moreover, including other sources of impedance that were not accounted for (e.g. pump ports, bellows, cross-section variations) should bring us to a more realistic impedance model. However, these contributions may be small. Subsequently, the use of full tracking codes (e.g. *Xsuite* [27]) will be considered to account for direct space-charge effects and study beam instabilities in the presence of impedance and space-charge.

ACKNOWLEDGEMENTS

Fermi Research Alliance, LLC manages and operates the Fermi National Accelerator Laboratory pursuant to Contract number DE-AC02-07CH11359 with the US DOE. This research was conducted as part of the Helen Edwards summer internship program at Fermi National Accelerator Laboratory.

REFERENCES

- [1] R. P. Stanek *et al.*, “PIP-II Project Overview and Status,” presented at SRF’23, Grand Rapids, MI, USA, Jun. 2023, paper MOIXA02, unpublished.
- [2] G. Jackson, “The Fermilab Recycler Ring Technical Design Report: Rev. 1.2,” 1996. doi:10.2172/16029
- [3] C. M. Bhat, “Proton Beam Intensity Upgrades for the Neutrino Program at Fermilab,” *PoS*, vol. ICHEP0216, p. 061, 2017. doi:10.22323/1.282.0061
- [4] B. C. Brown *et al.*, “The Fermilab Main Injector: High Intensity Operation and Beam Loss Control,” *Phys. Rev. Spec. Top. Accel. Beams*, vol. 16, no. 7, p. 071001, 2013. doi:10.1103/PhysRevSTAB.16.071001
- [5] D. S. Ayres *et al.*, “The NOvA Technical Design Report,” 2007. doi:10.2172/935497
- [6] R. Ainsworth *et al.*, “High intensity operation using proton stacking in the Fermilab Recycler to deliver 700 kW of 120 GeV proton beam,” *Phys. Rev. Accel. Beams*, vol. 23, no. 12, p. 121002, 2020. doi:10.1103/PhysRevAccelBeams.23.121002
- [7] R. Ainsworth, P. Adamson, J. Amundson, I. Kourbanis, Q. Lu, and E. Stern, “High intensity space charge effects on slip stacked beam in the Fermilab Recycler,” *Phys. Rev. Accel. Beams*, vol. 22, no. 2, p. 020404, 2019. doi:10.1103/PhysRevAccelBeams.22.020404
- [8] S. A. Antipov, P. Adamson, A. Burov, S. Nagaitsev, and M. J. Yang, “Fast Instability Caused by Electron Cloud in Combined Function Magnets,” *Phys. Rev. Accel. Beams*, vol. 20, no. 4, p. 044401, 2017. doi:10.1103/PhysRevAccelBeams.20.044401
- [9] A. Burov, “Convective Instabilities of Bunched Beams with Space Charge,” *Phys. Rev. Accel. Beams*, vol. 22, no. 3, p. 034202, 2019. doi:10.1103/PhysRevAccelBeams.22.034202
- [10] B. Salvant *et al.*, “Building the Impedance Model of a Real Machine,” in *Proc. IPAC’19*, Melbourne, Australia, May 2019, pp. 2249–2254. doi:10.18429/JACoW-IPAC2019-WEYPLS1
- [11] R. Wanzenberg, “Impedances and Instabilities,” in *CAS - CERN Accelerator School: Vacuum for Particle Accelerators*, 2020.
- [12] A. Macridin, “Transverse Impedance and Transverse Instabilities in the Fermilab Booster,” in *Proc. NAPAC’13*, Pasadena, CA, USA, Sep.-Oct. 2013, pp. 32–35. <https://jacow.org/PAC2013/papers/MOYBB2.pdf>
- [13] A. W. Chao, *Physics of collective beam instabilities in high-energy accelerators*. 1993.
- [14] L. Palumbo, V. G. Vaccaro, and M. Zobov, “Wake fields and impedance,” in *CERN Accelerator School: Course on Advanced Accelerator Physics (CAS)*, 1994, pp. 331–390. doi:10.5170/CERN-1995-006.331
- [15] D. A. Edwards and M. J. Syphers, *An Introduction to the Physics of High-Energy Accelerators*. Wiley, 1992.
- [16] K. Y. Ng, *Physics of intensity dependent beam instabilities*. 2006. doi:10.1142/5835
- [17] K. Y. Ng, “Betatron Tune Shifts and Laslett Image Coefficients,” 2001. doi:10.2172/783072
- [18] D. J. Larson, “A study of the heb longitudinal dynamics,” 1993. doi:10.2172/67778
- [19] K. Y. Ng, “Transverse instability at the recycler ring,” 2004. doi:10.2172/15020216
- [20] K. Y. Ng, “Physics of Intensity Dependent Beam Instabilities,” in *U.S. Particle Accelerator School (USPAS 2002)*, 2002.
- [21] M. Migliorati, L. Palumbo, C. Zannini, N. Biancacci, and V. G. Vaccaro, “Resistive wall impedance in elliptical multi-layer vacuum chambers,” *Phys. Rev. Accel. Beams*, vol. 22, no. 12, p. 121001, 2019. doi:10.1103/PhysRevAccelBeams.22.121001
- [22] J. Crisp and B. Fellenz, “Recycler short kicker beam impedance,” 2009. doi:10.2172/963777
- [23] K.-Y. Ng, “Impedances and beam stability issues of the Fermilab recycler ring,” 1996. doi:10.2172/237426
- [24] O. Mohsen, R. Ainsworth, and N. Eddy, “Waker Experiments at Fermilab Recycler Ring,” in *Proc. NAPAC’22*, Albuquerque, NM, USA, 2022, pp. 124–127. doi:10.18429/JACoW-NAPAC2022-MOPA33
- [25] A. Burov, Private communication.
- [26] IRIS, *IW2D*. <https://gitlab.cern.ch/IRIS/IW2D>
- [27] G. Iadarola *et al.*, “Xsuite: An Integrated Beam Physics Simulation Framework,” in *Proc. HB’23*, Geneva, Switzerland, Oct. 2023. doi:10.18429/JACoW-HB2023-TUA2I1